33rd Annual International Conference of the IEEE EMBS
Boston, Massachusetts USA, August 30 - September 3, 2011

Propagation of electrical field in the brain using electrical intra-cerebral stimulations

Janis Hofmanis, Valérie Louis-Dorr, Thierry Cecchin, *Member, IEEE*, Olivier Caspary, and Laurent Koessler

***Abstract*—For drug resistant partial epilepsy, intra-cerebral electrical stimulation (Deep Brain Stimulation - DBS) constitutes one of the means to locate epileptic volume. This paper investigates, in the framework of source localization problem, the propagation of the electrical field and current density distribution induced in the brain during *in vivo* electrical stimulation. There are three objectives in this work: to validate the propagation model for different large frequencies, to highlight the problem of the close field with the DBS source and to show the influence of the proximity to the skull on the results. We compared the Stereo-EEG data, recorded during DBS, with those obtained using: (i) the simplest model, the dipolar model in an infinite homogeneous medium, (ii) a more realistic approach with a numerical method, the Boundary Element Method (BEM). Studies on ten subjects with 234 stimulations showed that the dipole model could be used in the brain far from the skull in direction of dipole moment but that BEM was more appropriate close to the skull.**

I. INTRODUCTION

In pre-surgical evaluation for medically intractable epilepsy, Stereo-EEG (SEEG) is used to determine the irritative and epileptogenic zones. To facilitate the delimitation of these zones and establish a functional cerebral cartography of the anatomic structures, an intra-cerebral electrical stimulation (Deep Brain Stimulation - DBS) can be used to test functional cerebral areas and to reproduce the usual epileptic seizures. This exogenous source can thus activate the epileptic networks under unclaimed and generate an electrophysiological reaction. Then, brain source imaging can be used to localize the epileptogenic source by solving the forward problem. In this context, the notion of generated dipole due to the synchronized synaptic current was introduced in 1981 by Nunez [1] and reinforced by Niedermeyer and Lopes Da Silva in 1998 [2]. The current propagated in the brain is the consequence of this process in the Klee *et al.* and Creutzfeldt *et al.* demonstrations and the relationship between intracellular cortical neurons and EEG activities [3], [4]. The electric potential and magnetic field in the space depends on the conductive current source distribution of the head and on the conductive properties of tissues. The dipolar model applied in an infinite homogeneous medium was the simplest approach to solve the forward problem however more and more complex propagation models were developed for the estimation of the scalp potentials and electric fields. These models use numerical methods and realistically shaped head model: Boundary Element Method (BEM), Finite Element Method (FEM), and Finite Difference Method (FDM) [5], [6].

The DBS propagates itself in the brain and these attenuated harmonics can be viewed in the SEEG signals. Then, the analysis of the SEEG signals during the stimulation could be a way to investigate the bioelectric phenomena in the brain *in vivo* taking into account the influence of several parameters: (i) the frequency of the source (due to its square waveform, the stimulation source is composed of several harmonics at different frequencies), (ii) the distance to the source and the position inside the brain (the coordinates of the measurement contacts of SEEG electrodes were known using a stereotactic CT-scan).

In this paper, we compared the behavior of SEEG data during DBS with a simplified model that assumes an infinite homogenous and isotropic medium, and the BEM. In the next section, we present the theoretical background. The patients' data, the characteristics of the DBS and the SEEG recording are then described in the third section. In the fourth section, we show and discuss the results obtained with 234 stimulations.

II. THEORETICAL BACKGROUND

The post-synaptic potentials have duration of about 10 ms. As a consequence, the time frequencies of the brain electromagnetic field can rarely exceed 100 Hz in the scalp. Therefore the time derivatives in Maxwell's equations can be neglected; this is called the quasi-static approximation [1], [7], [8]. Let us consider $\mathbf{J}^p$, the primary current density that reflects the brain electrical activity. The current of the single dipole at position $\boldsymbol{r}_0$ ($\boldsymbol{r}_0 \in \mathbb{R}^3$) with a moment $\boldsymbol{I}$ can be written, at position $\boldsymbol{r}$:

$$\boldsymbol{J}^p(\boldsymbol{r}) = \delta_{\boldsymbol{r}0}\boldsymbol{I} \quad (1)$$

where δ is the Dirac distribution and $\delta_{\boldsymbol{r}0} = \delta(\boldsymbol{r} - \boldsymbol{r}_0)$ [5]. Furthermore, if the volume (called vol), can be considered small compared to the distance to $\boldsymbol{r}$, then the potential field in an infinite, homogeneous and isotropic medium is:

$$V(\mathbf{r}) = \frac{1}{4\pi\sigma}\int_{vol}\mathbf{J}^p(\mathbf{r}')\frac{(\mathbf{r}-\mathbf{r}')}{\|\mathbf{r}-\mathbf{r}'\|^3}dr' \approx \frac{1}{4\pi\sigma}\mathbf{I}\frac{(\mathbf{r}-\mathbf{r}_0)}{\|\mathbf{r}-\mathbf{r}_0\|^3} \quad (2)$$

This study was supported by the French Ministry of Health (PHRC 17-05, 2009). J. Hofmanis, V. Louis-Dorr, T. Cecchin and O. Caspary works for the Centre de Recherche en Automatique de Nancy (CRAN), Nancy-Université, CNRS (janis.hofmanis@ensem.inpl-nancy.fr, valerie.louis@ensem.inpl-nancy.fr, tcecchin@iutsd.uhp-nancy.fr, ocaspary@iutsd.uhp-nancy.fr). L. Koessler works for the CRAN, Nancy-Université, CNRS and Centre Hospitalier Universitaire de Nancy (l.koessler@chu-nancy.fr).

where σ is the conductivity. Besides, for the usual dipole with source I and sink $-I$ separated by a distance d considered small compared to the distance to $\mathbf{r}$, then the potential field in an infinite, homogeneous and isotropic medium is:

$$V(\mathbf{r}) \approx \frac{I}{4\pi\sigma} \frac{(\mathbf{r}-\mathbf{r}_0)}{\|\mathbf{r}-\mathbf{r}_0\|^3} \quad (3)$$

According to [1], for distance $r = \|\mathbf{r}-\mathbf{r}_0\|$ greater than about $3d$ or $4d$, we can write an approximation of (3) like:

$$V(\mathbf{r}) \approx \frac{I\cos(\theta)}{4\pi\sigma r^2} \quad (4)$$

where θ represents the angle between the dipole axis and the vector r to the point of the measurement.

Obviously, the head is not an infinite conductor and three-dimensional (3-D) spatial analysis of EEG requires accurate knowledge of the electrical properties of head tissues like geometrical, homogeneous and isotropic layers and structures [9]-[11]. In a simplified approach and the BEM implementations, generally, the three-shell model of the head (scalp, skull, brain) is used and the tissues are segmented and matched in the 3D IRM. The point is to estimate the electrical potential field caused by a known distribution of current sources in a piecewise homogeneous volume conductor model of the head [12]. Then, the integral equation of the potential takes into account various media conductivities. Although Logothetis *et al.* [13] highlight the measurements in the monkeys' brains, the impedance of which is independent of frequency, is homogeneous and tangentially isotropic within gray matter, and can be theoretically predicted assuming a pure-resistive conductor.

III. Materials and Methods

A. Patients data and stereotactic placement of intracerebral electrodes

Ten drug-resistant partial epilepsy patients (5 males, 5 females, average age: 37 years old) were included in this retrospective study. The electrode implantation sites were chosen according to non-invasive data collected during the earlier pre-surgical phase. In the overall population, six patients had temporal lobe epilepsy, two had posterior cortex epilepsy, one had frontal lobe epilepsy and one had central epilepsy. From 8 to 13 electrodes (Dixi Medical, Besançon, France), consisting of 5−18 contiguous contacts were placed in the brain (Fig. 1). Stereotactic placement of the electrodes was performed as follows: a stereotactic MRI (3D SPGR T1 weighted-sequence, voxel size 1.2*1.2*1.2) was carried out and electrode trajectories were calculated according to pre-operative planning with careful avoidance of vascular structures. After induction of general anesthesia, the Leksell G-frame (Elekta S.A, Stockholm, Sweden) was positioned on the patient's head and electrodes were implanted. A post-operative stereotactic CT-scan was then performed and automatically fused with pre-operative MRI to determine the exact position of each electrode [14].

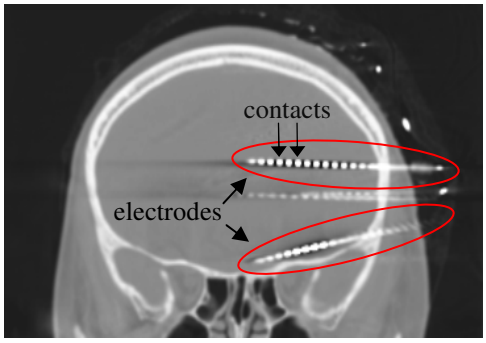

Fig. 1 Depth electrodes implantation.

B. Electrical stimulation and SEEG recording

The stimulation was applied between two contiguous contacts at different levels along the axis of several intracerebral electrodes. It was composed of a series of biphasic impulsions (Fig. 2) for 3-10 s with intensity between 0.2 to 3 mA.

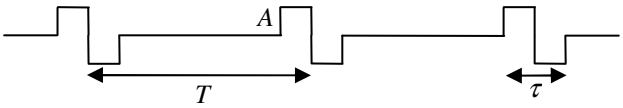

Fig. 2. The electrical stimulation. T = 20 ms, τ = 1 ms.

The frequency spectrum (Fig. 3) of this periodic signal was discrete and the amplitude A_k of the k-th harmonic was:

$$A_k = 2A\frac{\tau}{T}\left|\mathrm{sinc}(k\frac{\tau}{2T})\sin(k\frac{\pi\tau}{2T})\right| \quad (5)$$

where A is the magnitude of the stimulation, τ the width of the biphasic impulsion and T the period of the impulsion.

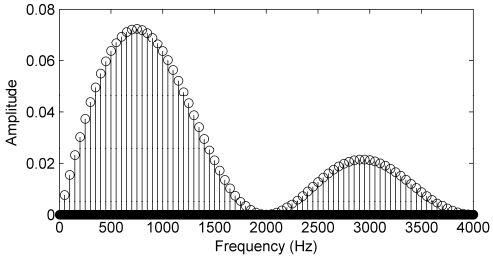

Fig. 3. Theoretical frequency spectrum of the stimulation in the range 0-4000 Hz. The stimulation magnitude was 1.

SEEG and video monitoring were performed 24 h/day for 4 days. For SEEG signals, the reference was chosen on the surface of the head. The signals were digitized at a 4096 Hz sampling rate on a 128 channel amplifier (LTM 128 Headbox; Micromed, Italy) and decimated to be recorded at 512 Hz. Two anti-aliasing filters were used: a hardware filter before digitization at 4096Hz and a digital filter before decimation. These filters were designed according to the bandwidth of the EEG signal but they were not selective enough to suppress the harmonics of the stimulation signal higher than the final Nyquist frequency. As a consequence, aliasing occurred (Fig. 4).

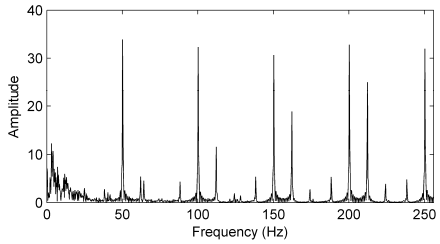

Fig. 4. Frequency spectrum of the signal recorded on a SEEG contact during a stimulation. We can see the fold harmonics of fundamental frequency (50 Hz) up to 1000 Hz.

C. *Choice of the excitation frequencies*

The presence of harmonics in the frequency band of the sampled signal (0-256 Hz) allowed studying their propagation in the brain. We were particularly interested in the range 0-500 Hz to take into account high-frequency oscillations [15]. The power supply frequency (50 Hz) and the first odd harmonic (150 Hz) were not kept because the magnitude of the power supply noise was too high for these frequencies. Moreover, we also eliminated the 500 Hz frequency because its fold frequency (12 Hz) was situated in the α-rhythm band. Then, the following frequencies were selected: 100, 200, 250, 300, 350, 400, 700, 750, 800 Hz.

IV. Results and Discussion

A. *Analysis of the frequency influence*

To analyze the effects of the stimulation frequency on intracranial electrical propagation, we selected 234 stimulations (average of 109 contacts/measurements per stimulation). Fig. 5 presents the distribution of harmonic frequencies according to the stimulation distance.

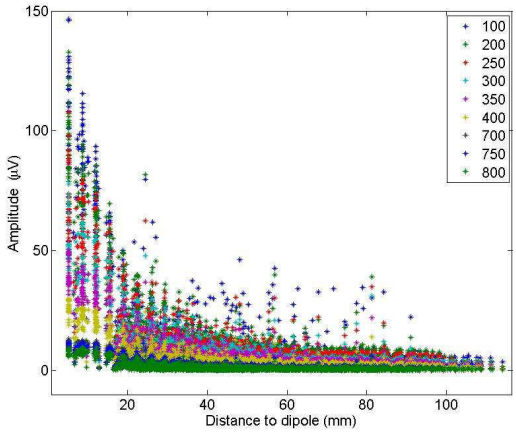

Fig. 5. Amplitudes of harmonic frequencies by distance.

To free itself from the variation of: (i) the stimulation current, (ii) the harmonics amplitude (due to input signal level and anti-aliasing filter attenuation), the amplitude values were normalized by the values of the frequency with the highest selected frequency amplitude (after anti-aliasing filtering and decimation): 200 Hz (Fig. 6). We noticed that, except for the small distances, the normalized values were roughly constant for each frequency. Then, we assumed that the brain conductivity does not change with the distance, whatever the frequency. The variation of the normalized frequencies at the first millimeters may be due to the contacts of the stimulating electrode which seemed to have a particular trend (Fig. 7). This could be due to a close distributed dipole field or to a stimulating electrode artifact.

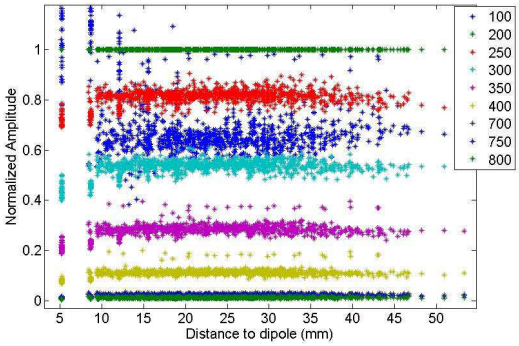

Fig. 6. Normalized Amplitudes by distance for different harmonics (100 – 800) Hz.

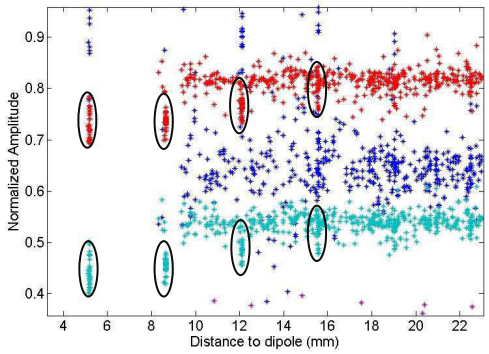

Fig. 7. Normalized frequencies of 250 Hz (red) and 300 Hz (cyan) for small distances to the stimulation. Measurements acquired by other contacts of stimulated electrode are pointed out with black ellipses.

B. *Analysis of the boundaries effects*

Considering the stimulation as a dipole source in a closed volume media, the boundaries of the head had to be taken into account. In the model of a point dipole (Fig. 8) we notice an unsymmetrical decrease of the potential at both sides of the dipole, if it is near the boundary skull. The same observations can be made for a set of nested volumes as brain, skull and scalp, with two different conductivities.

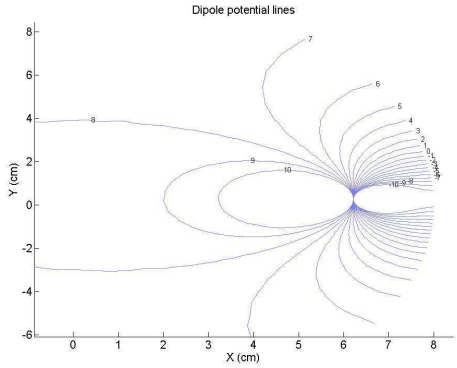

Fig. 8. Potential lines of a point dipole in conductive closed volume. The potential lines are unsymmetrical due to the proximity of the boundary (in the right side of the graph).

As an illustration of the boundary effect, in Fig. 9 (b), we

compared 100 Hz frequency amplitudes with the dipole model given in (4) and BEM lead field calculated by OpenMEEG [16] for the contacts of the electrode G' (Fig. 9 (a) - blue) when 3rd and 4th contacts of the electrode I' (Fig. 9 (a) - red) were stimulated. The BEM results were closer to the experimental data than those obtained with the dipole model.

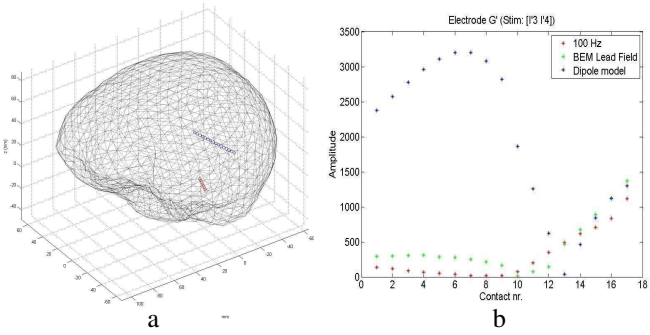

Fig. 9. a) Placement of two electrodes (blue – G', red – I') inside a brain. b) Amplitude of 100 Hz frequency, BEM lead field and approximated dipole model (normalized by mean value of 100 Hz frequency) for G' electrode (17 contacts). 1 – far (deep) from skull, 17 – close to skull.

C. *Dipole model fitting*

To validate the dipole model propagation law, for each frequency and for each patient, we divided the measured amplitudes by the absolute value of the cosine of θ, the angle between the dipole axis and the vector **r** to the point of the measurement. This ratio was computed for several intervals of θ so that we can assume, under the assumption that (5) is verified, that the resulting points could be fitted by an a/r^2 distribution where a is a constant and r the distance between the dipole center and the considered measurement contact. Then, we fitted these obtained points with a basic nonlinear least squares fit function of the form $a/r^2 + b$ (we added a constant term b to take the noise into account). Globally, the experimental data fitted the model except near the skull.

Fig. 10 is an example of such a fitting. It shows the measurements, for one patient, in which the absolute cosine of the angle with stimulating dipole is higher than 0.7, and without the first three closest contacts of the stimulating electrode in order to avoid the problem of artifact described in part *B*.

V. Conclusion

In this paper we presented preliminary results on the use of the DBS in order to compare, *in vivo*, the dipole model and the BEM. This was a retrospective study and, for future study, we propose to modify the fundamental frequency of the stimulation to access frequency lower than 100 Hz. Our objective is to estimate the anisotropy of conductivity in white matter and other cerebral structures, taking the whole parameters into account.

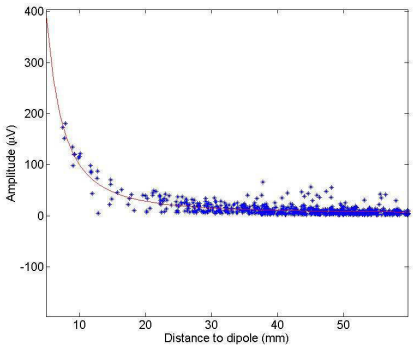

Fig. 10. Amplitude of 100 Hz frequency (blue points) and fitted model (red line) for one patient.

References

[1] P. L. Nunez, *Electric Fields of the Brain: The Neurophysics of EEG*. Oxford: Oxford University Press, 1981.

[2] E. Niedermeyer, and F. Lopes da Silva, Ed. *Electroencephalography*. Baltimore, MD: Williams and Wilkins, 1998.

[3] M. R. Klee, K. Offenloch, and J. Tigges, "Cross-correlation analysis of electroencephalographic potentials and slow membrane transients," *Science*, vol. 147, pp. 519–521, 1965.

[4] O. T. Creutzfeld, S. Watanabe, and H. D. Lux, "Relations between EEG phenomena and potentials of single cortical cells. II. Spontaneous and convulsoid activity," *Electroenceph. Clin. Neurophysiol.*, vol. 20, pp. 19–37, 1966.

[5] S. Vallaghé "EEG and MEEG forward modeling: computation and calibration," Ph.D. Thesis, Université de Nice Sophia Antipolis, 2008.

[6] H. Hallez, B. Vanrumste, R. Grech, J. Muscat, W. De Clercq, A. Vergult, Y. D'Asseler, K. P. Camilleri, S. G. Fabri, S. Van Huffel, and I. Lemahieu, "Review on solving the forward problem in EEG source analysis", *Journal of NeuroEnginering and Rehabilitation*, vol. 4, 2007.

[7] C. A. Bossetti, M. J. Birdno, and W. M. Grill, "Analysis of the quasi-static approximation for calculating potentials generated by neural stimulation," *Journal of Neural Engineering*, vol. 5, pp. 44-53, 2008.

[8] M. Hamalainen, R. Hari, R. J. Ilmoniemi, J. Knuutila, and O. V. Lounasmaa, "Magnetoencephalography – Theory, instrumentation, and applications to noninvasive studies of the working human brain," *Rev. Mod. Phys.*, vol. 65, pp. 413–498. 1993.

[9] K. A. Awada, D. R. Jackson, S. B. Baumann, J. T. Williams, D. R. Winton, P. W. Fink, and B. R. Prasky, "Effect of conductivity uncertainties and modeling errors on EEG source localization using a 2-D model," *IEEE Trans. Biomed. Eng.*, vol. 45, pp. 1135–1145, 1998.

[10] J. Haueisen, C. Ramon, M. Eiselt, H. Brauer, and H. Nowak, "Influence of tissue resistivities on neuromagnetic fields and electric potentials studied with a finite element model of the head," *IEEE Trans. Biomed. Eng.*, vol. 44, pp. 727–735, 1997.

[11] T. C. Ferree, K. J. Eriksen, and D. M. Tucker, "Regional head tissue conductivity estimation for improved EEG analysis," *IEEE Trans. Biomed. Eng.*, vol. 47, pp. 1584–1592, 2000.

[12] D. B. Geselowitz, "On bioelectric potentials in an inhomogeneous volume conductor," *Biophys. J.*, vol. 7, pp. 1–11, 1967.

[13] N. K Logothetis, C. Kayser, and A Oeltermann, "In vivo measurement of cortical impedance spectrum in monkeys: implication for signal propagation," *Neuron*, vol. 55, pp. 809–823, 2007.

[14] J. Hofmanis, V. Louis-Dorr, O. Caspary, and L. Maillard, "Automatic depth electrode localization in intracranial space," in *Proc. 4th Int. Joint Conf. on Biomedical Engineering Systems and Technologies*, Rome, 2011.

[15] E. Urrestarazu, R. Chander, F. Dubeau, and J. Gotman, "Interictal high-frequency oscillations (100-500Hz) in the intracerebral EEG of epileptic patients," *Brain*, vol. 130, pp. 2354–2366, 2007.

[16] A. Gramfort, T. Papadopoulo, E. Olivi, and M. Clerc, "Forward Field Computation with OpenMEEG," *Computational Intelligence and Neuroscience*, vol. 2011, 13 pages, 2011.